X-ray/Neutron Diffraction and Electrochemical Studies of Lithium De/Re-Intercalation in $Li_{1-x}Co_{1/3}Ni_{1/3}Mn_{1/3}O_2$ ($x = 0 \rightarrow 1$)

S.-C. Yin,[†] Y.-H. Rho,[†] I. Swainson,[‡] and L. F. Nazar*[,†]

Department of Chemistry, University of Waterloo, Waterloo, Ontario, Canada N2L 3G1, and Chalk River Laboratories, Chalk River, Ontario, Canada K0J 1J0

Received June 1, 2005. Revised Manuscript Received February 1, 2006

X-ray and neutron diffraction studies were carried out on highly ordered (2−3% Li/Ni exchange) layered $Li_{1-x}Co_{1/3}Ni_{1/3}Mn_{1/3}O_2$ [$(1 - x) = 1.0$; 0.8, 0.6, 0.45, 0.30, 0.04] prepared by chemical delithiation and relithiation. The studies reveal that the initial $R\bar{3}m$ phase (O3) is maintained up to extraction of 0.70−0.75 Li and exhibits only ∼1% change in volume over the range of composition. Additional extraction of Li results in the appearance of the O1 phase (trigonal; $P3m1$), which displays a strong contraction in the *c* axis by 5.3% and a volume decrease of 7.2%. Oxygen vacancies were not evident in the completely delithiated material. Re-intercalation of lithium in this phase was relatively irreversible, however, resulting in poorly defined mixtures of the O3 and O1 structures that exhibited a large fraction of stacking faults. In contrast, materials that were not delithiated beyond $x = 0.30$ resulted in fully reversible reformation of the original crystalline O3 phase on re-intercalation. Electrochemical cycling under different cutoff voltages were in accord with these observations and suggest an optimum upper cutoff voltage of 4.3−4.4 V.

Introduction

Layered alkali transition metal oxides such as $LiCoO_2$ and $Na_{0.7}CoO_2$ have inspired much interest this past decade owing to their diverse properties that range from superconductivity to facile electron and ion transport. The latter properties make $LiCoO_2$ the cathode of choice in virtually all lithium-ion cells today. Following its first investigation by Goodenough et al.[1] and implemention by SONY, it has dominated the market due to its high energy density and cycling stability. Nonetheless, the high cost of cobalt, together with safety issues that arise as a consequence of the electronic structure of $LiCoO_2$, has driven worldwide efforts to find alternatives. Ideally, these would be lithium metal oxides that replace the Co partially or completely with more economically viable transition metals such as Ni or Mn, to meet future demands of large scale batteries for electric vehicles but still maintain the benefits of excellent electrochemical behavior.

This search has led to various promising materials based on the layered oxide or "ordered rock salt" structure. The first to be studied focused on substitution of $LiNiO_2$,[2,3] such as $Li[Al_xCo_{1-y}Ni_{1-x-y}O_2]$, which is a potential commercial candidate developed in conjunction with the SAFT company. $LiNiO_2$ suffers thermal stability issues and impeded Li transport by extra Ni in the Li layer, but partial substitution improves the properties significantly. The concept of "doping" of the Co within the layers extends to variations of multiple transition metal solid solutions, such as $LiCo_{1-x}Ni_xO_2$ ($0 \leq x \leq 1$)[1,4,5] and $LiNi_xCo_{1-2x}Mn_xO_2$ ($0 \leq x \leq 1/2$),[6] and the potential line phases $LiNi_{1/2}Mn_{1/2}O_2$[7] and $LiCo_{1/3}Ni_{1/3}Mn_{1/3}O_2$.[8] Layered metal oxides containing lithium within the transition metal layers have also been examined in detail, including $Li[Ni_xLi_{1/3-2x/3}Mn_{2/3-x/3}]O_2$ ($0 \leq x \leq 1/2$)[9] and $Li[Li_{0.2}Cr_{0.4}Mn_{0.4}]O_2$.[10−12] Among these materials, $LiCo_{1/3}Ni_{1/3}Mn_{1/3}O_2$ was reported to have capacity comparable to or higher than $LiCoO_2$ and better thermal stability,[13] which are requirements for large scale rechargeable batteries under demanding conditions. Initial reports suggested capacities of up to 190−220 mA h g^{-1}, albeit in a wide voltage window[8] (2.5−5.0 V). Many subsequent studies have also demonstrated its good capacity even at moderately high rates.[14−17]

* To whom correspondence should be addressed. E-mail: lfnazar@uwaterloo.ca.
[†] University of Waterloo.
[‡] Chalk River Laboratories.

(1) Mizushima, K.; Jones, P. C.; Wiseman, P. J.; Goodenough, J. B. *Mater. Res. Bull.* **1980**, *15*, 783.
(2) Dahn, J. R.; von Sacken, U.; Juskow, M. W.; Al-Janabi, J. *J. Electrochem. Soc.* **1991**, *138*, 2207.
(3) Delmas, C.; Saadoune, I.; Rougier, A. *J. Power Sources* **1993**, *43/44*, 595.
(4) Dahn, J. R.; von Sacken, U.; Michal, C. A. *Solid State Ionics* **1990**, *44*, 87.
(5) Ohzuku, T.; Ueda, A.; Nagayama, M.; Iwakoshi, Y.; Komori, H.; *Electrochim. Acta* **1993**, *38*, 1159.
(6) Lu, Z.; MacNeil, D. D.; Dahn, J. R. *Electrochem. Solid-State Lett.* **2001**, *4*, A200.
(7) Ohzuku, T.; Makimura, Y. *Chem. Lett.* **2001**, 744.
(8) Ohzuku, T.; Makimura, Y. *Chem. Lett.* **2001**, 642.
(9) Lu, Z.; MacNeil, D. D.; Dahn, J. R. *Electrochem. Solid-State Lett.* **2001**, *4*, A191.
(10) Storey, C.; Kargina, I.; Grincourt, Y.; Davidson, I. J.; Yoo, Y.; Seung, D. Y. *J. Power Sources* **2001**, *97*−*98*, 541.
(11) Grincourt, Y.; Storey, C.; Davidson, I. J. *J. Power Sources* **2001**, *97*−*98*, 711.
(12) Ammundsen, B.; Paulsen, J.; Davidson, I.; Liu, R.-S.; Shen, C.-H.; Chen, J.-M.; Jang, L.-Y.; Lee, J.-F. *J. Electrochem. Soc.* **2002**, *149*, A431.
(13) Ohzuku, T.; Yabuuchi, N. *J. Power Sources* **2003**, *119*, 171.
(14) Belharouak, I.; Sun, Y.-K.; Liu, J.; Amine, K. *J. Power Sources* **2003**, *123*, 247.
(15) Lee, M.-H.; Kang, Y.-J.; Myung, S.-T.; Sun, Y.-K. *Electrochim. Acta* **2004**, *50*, 939.
(16) Cho, T. H.; Park, S. M.; Yoshio, M.; Hirai, T.; Hideshima, Y. *J. Power Sources* **2005**, *142*, 306.

10.1021/cm0511769 CCC: $33.50
Published on Web 03/07/2006

$LiCo_{1/3}Ni_{1/3}Mn_{1/3}O_2$ can be considered as a 1:1:1 solid solution between $LiCoO_2$, $LiNiO_2$, and $LiMnO_2$[18] or a 1:2 solid solution between $LiCoO_2$ and $LiNi_{1/2}Mn_{1/2}O_2$ ($LiCo_{1-2x}Ni_xMn_xO_2$).[19] It crystallizes in the ordered rock salt α-$NaFeO_2$-type structure ($R\bar{3}m$), isostructural with the pure cobalt and nickel compounds. The *c* axis in the unit cell of this "O3" phase comprises three MO_2 sheets.[20] The structure can also be deemed an ordered rock salt, in which lithium oxide and metal oxide layers alternate along the [111] direction.[21] Any mixing of the Li ions and metal cations between the two layers hence forms a "disordered" rock salt structure. The degree of disorder is related to the extent of cation exchange, which is thought to occur solely between Ni^{2+} (0.69 Å) and Li^+ (0.76 Å), as a result of their similarity in size. The disorder ranges up to ∼10% in $LiNi_{1/2}Mn_{1/2}O_2$[22] to lower than ∼5% in $LiCo_{1/3}Ni_{1/3}Mn_{1/3}O_2$. Its role is not fully understood in determining electrochemical behavior. In $LiNiO_2$, as little as 2% Ni in the Li layer decreases the cycling life very significantly.[23,24] In $LiNi_{1/2}Mn_{1/2}O_2$, the extensive cation exchange leads to the ordering of Li, Ni, and Mn within the metal layers,[25,26] as demonstrated by nuclear magnetic resonance (NMR) and first-principle calculations.[27] Despite this (or because of it), a decrease in the rate of Li extraction is observed for this material.[28] Cobalt substitution decreases the degree of cation disorder, and this has been attributed to the increase in the rate of Li extraction in $LiCo_{1-2x}Ni_xMn_xO_2$.

Despite studies showing the superior capacity and cyclability of $LiCo_{1/3}Ni_{1/3}Mn_{1/3}O_2$,[14,29,30] changes in its structure after deep Li extraction have not been examined and nor are its cycling properties and structural stability at high cutoff voltages fully understood. A slight stoichiometric excess of lithium was recently found to be beneficial to cycling behavior; however, cracking in the electrode mixture occurred at cutoff voltages >4.6 V.[31] Here, we use neutron diffraction to examine the changes in the structure upon chemical delithiation and relithiation, which is similar (albeit not identical) to electrochemical cycling at intermediate rates (∼2 C).[28] We show that the fully delithiated structure $Li_{0.04}Co_{1/3}Ni_{1/3}Mn_{1/3}O_2$ forms an O1 phase, composed of one MO_2 layer along *c* axis of the unit cell. After full extraction, the *c* axis of the cell, which is parallel to the layer stacking direction, contracts as much as 5.3%, and the cell volume is decreased by 7.2%. Such structural changes lead to the irreversibility of conversion of the O1 structure back to the pristine O3 structure on discharge and may be responsible for cracking of the electrode composite. Factors such as particle morphology are discussed with respect to the extent of the O1 phase formation, which is associated with the upper cutoff voltage.

Experimental Section

Sample Preparation. Layered $LiCo_{1/3}Ni_{1/3}Mn_{1/3}O_2$ compounds were prepared by the mixed hydroxide method. Stoichiometric amounts of $Co(NO_3)_2 \cdot 6H_2O$ (Fisher), $Ni(NO_3)_2 \cdot 6H_2O$ (Alfa), and $Mn(NO_3)_2$ (Fisher, 50% solution) were mixed in deionized water and added dropwise into a 1 M LiOH solution via a buret. The resultant precipitates were filtered and washed with deionized water to remove LiOH. The washed precipitates were dried at 150 °C overnight prior to being mixed with a stoichiometric amount of $LiOH \cdot H_2O$. Materials were preheated at 480 °C for 3 h, calcined at 1000 °C for 3 h, and subsequently air cooled at intermediate rates (∼5 °C/min). Chemical analysis of the Li, Co, Ni, and Mn contents was performed using inductive coupled plasma (ICP) spectroscopy, and determination of the oxidation state (oxygen content) was carried out by iodometric titration.[32]

Chemical Delithiation and Relithiation. In an Ar filled glovebox, 2 g of $LiCo_{1/3}Ni_{1/3}Mn_{1/3}O_2$ was mixed with the desired ratio of NO_2BF_4 in 200 mL of acetonitrile and stirred for 1 day before being filtered. Relithiation experiments were carried out by reaction of the material with designated quantities of LiI in an acetonitrile solution for 1 day. All samples were washed three times with acetonitrile to remove remaining salts. Li stoichiometries of these samples were obtained from ICP analysis.

Powder Neutron Diffraction (PND). About 2 g of material was loaded in a vanadium can in an Ar filled glovebox. Patterns were collected over a 12 h period on the C2 constant wavelength (λ = 1.327 78 Å) powder diffractometer at Chalk River Laboratories, Canada, in the conventional Debye−Scherrer mode. Si powder (NIST 640c) was used as an external calibration standard in a vanadium can and measured in the same configuration as the sample. The can was centered by means of a dial gauge on the stage.[33] Measurements were carried out from 5 to 116° in 2θ at 300 K, using a step size of 0.1°.

Powder X-ray Diffraction. Samples were measured on a Bruker D8 Advance powder diffractometer using standard Bragg−Brentano geometry with Cu Kα radiation (λ = 1.5406 Å). Data were collected from 10 to 102° in 2θ, using a step size of 0.02° and a count time of 10 s. Air-sensitive samples were placed in a holder with a Kapton window and measured on a Siemens D500 powder diffractometer.

Rietveld Analysis. Powder neutron or X-ray data sets were both refined using the GSAS package with the EXPGUI interface.[34] Backgound, scale factor, zero point, lattice parameters, atomic positions, and coefficients for the peak shape function were iteratively refined until convergence was achieved. The total number of variables for the neutron refinements of $Li_xCo_{1/3}Ni_{1/3}Mn_{1/3}O_2$

(17) Park, S.-H.; Shin, H.-S.; Myung, S.-T.; Yoon, C. S.; Amine, K.; Sun, Y. K. *Chem. Mater.* **2005**, *17*, 6−8.
(18) Koyama, Y.; Makimura, Y.; Tanaka, I.; Adachi, H.; Ohzuku, T. *J. Electrochem. Soc.* **2004**, *151*, A1499.
(19) Lu, Z.; MacNeil, D. D.; Dahn, J. R. *Electrochem. Solid-State Lett.* **2001**, *4*, A200.
(20) Delmas, C.; Fouassier, C.; Hagenmuller, P. *Physica* **1980**, *99B*, 81.
(21) Mather, G. C.; Dussarrat, C.; Etourneau, J.; West, A. R. *J. Mater. Chem.* **2000**, *10*, 2219.
(22) Lu, Z.; Beaulieu, L. Y.; Donaberger, R. A.; Thomas, C. L.; Dahn, J. R. *J. Electrochem. Soc.* **2002**, *149*, A778.
(23) Peres, J. P.; Delmas, C.; Rougier, A.; Broussely, M.; Perton, F.; Biensan, P.; Willmann, P. *J. Phys. Chem. Solids* **1996**, *57*, 1057.
(24) Rougier, A.; Gravereau, P.; Delmas, C. *J. Electrochem. Soc.* **1996**, *143*, 1168.
(25) Meng, Y. S.; Ceder, G.; Grey, C. P.; Yoon, W.-S.; Shao-Horn, Y. *Electrochem. Solid-State Lett.* **2004**, *7*, A155.
(26) Meng, Y. S.; Ceder, G.; Grey, C. P.; Yoon, W.-S.; Jiang, M.; Breger, J.; Shao-Horn, Y. *Chem. Mater.* **2005**, *17*, 2386.
(27) Yoon, W.-S.; Iannopollo, S.; Grey, C. P.; Carlier, D.; Gorman, J.; Reed, J.; Ceder, G. *Electrochem. Solid-State Lett.* **2004**, *7*, A167.
(28) Venkatraman, S.; Choi, J.; Manthiram, A. *Electrochem. Commun.* **2004**, *6*, 832.
(29) Hwang, B. J.; Tsai, Y. W.; Carlier, D.; Ceder, G. *Chem. Mater.* **2003**, *15*, 3676.
(30) Shaju, K. M.; Subba Rao, G. V.; Chowdari, B. V. R. *Electrochim. Acta* **2002**, *48*, 145.
(31) Choi, J.; Manthiram, A. *Electrochem. Solid-State Lett.* **2004**, *7*, A365.
(32) Karppinen, M.; Matvejeff, M.; Salomski, K.; Yamauchi, H. *J. Mater. Chem.* **2002**, *12*, 1761.
(33) Larson, A. C.; Von Dreele, R. B. *GSAS*; Technical Report NM87545; Los Alamos National Laboratory: Los Alamos, NM, 1994.
(34) Toby, B. H. *EXPGUI*, a graphical user interface for *GSAS*. *J. Appl. Crystallogr.* **2001**, *34*, 210−213.

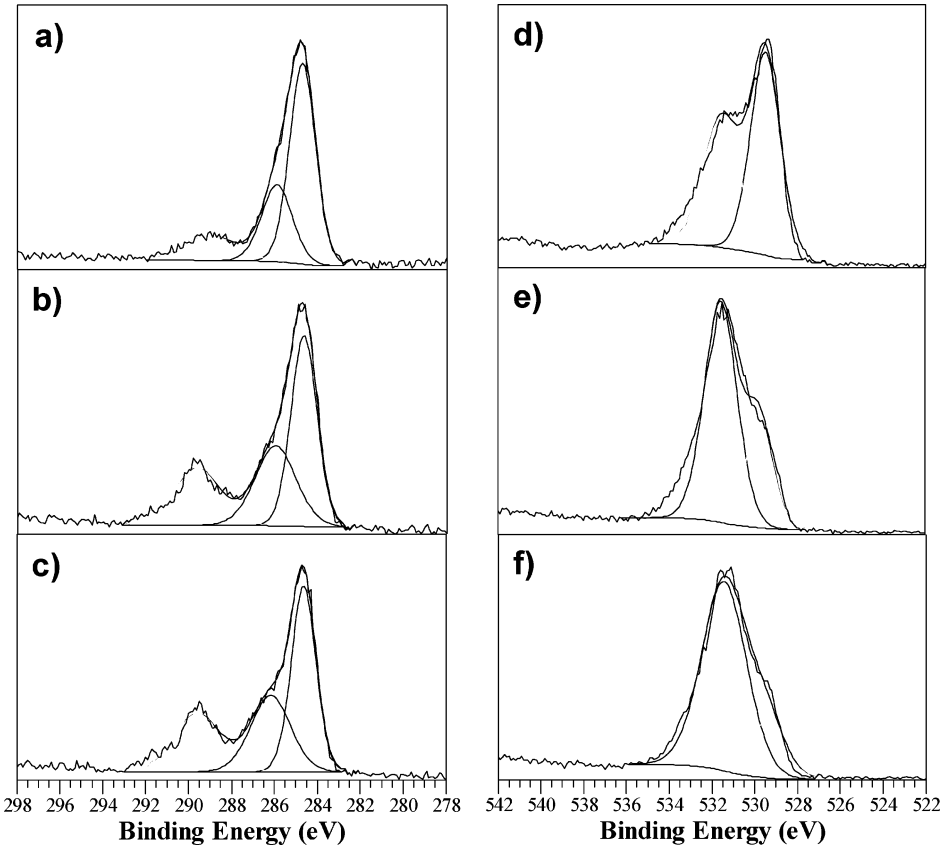

Figure 1. XPS spectra for compositions A, B, and C as described in the text: C 1s XPS are shown in parts a−c, respectively; O 1s spectra are shown in parts d−f, respectively.

compositions ($x = 1.00$, 0.84, 0.60, 0.52, 0.45, and 0.04) were 22, 23, 23, 23, 23, and 22, respectively. Details on the occupancy and thermal factor constraints applied in the refinement are listed in the relevant tables.

Scanning Electron Microscopy. Samples were gold coated and examined in a LEO 1530 field-emission scanning electron microscopy (FESEM) microscope instrument equipped with an energy-dispersive X-ray (EDX) spectroscopy attachment. Images were recorded at 15 kV with a secondary electron detector.

Electrochemistry. Cathode mixtures were composed of 84% (or 76%) active material, 8% (or 16%) Super S carbon as the conductive additive, and 8% Kynar-Flex as the binder. The mixture was dispersed in *N*-methylpyrrolidinone and doctor blade-coated onto an aluminum foil current collector. The cathode disks were punched from the foil, pressed under three tons of pressure, and dried in a vacuum oven at 120 °C. Type 2220 coin cells were assembled in an Ar filled glovebox using metal lithium as the anode, Celgard separators, and a mixture of 1 M $LiPF_6$ in ethylene carbonate (EC)/dimethyl carbonate (DMC) as the electrolyte. Cells were run at constant current at a C/10 rate (equivalent to a current density of 5 mA/g) in the 3.0/4.5 V or 2.5/4.4 V window using a MacPile controller (Biologic S.A., Claix, France).

X-ray Photoelectron Spectroscopy (XPS). Materials were analyzed with a VG Scientific XPS Microprobe ESCALab 250 using focused monochromatic Al Kα radiation (1486.6 eV). Samples were deposited on a Cu substrate with an irradiated area of 0.4×1 mm^2 and loaded in the chamber at a pressure of less than 10^{-10} mbar. The spectral peaks were deconvoluted by CasaXPS software.

Results and Discussion

I. $LiCo_{1/3}Ni_{1/3}Mn_{1/3}O_2$ Compositions: Analysis. Prior to carrying out diffraction studies, the mixed metal oxide was characterized thoroughly in terms of content. Three "$LiCo_{1/3}Ni_{1/3}Mn_{1/3}O_2$" compositions were prepared (A, B, and C), that differed in terms of apparent lithium "overstoichiometry". The presence of additional lithium in $Li_{1+x}MO_2$ metal oxides is not well-understood but has recently been reported to be advantageous for the electrochemical properties of $Li_{1+x}Co_{1/3}Ni_{1/3}Mn_{1/3}O_2$.[35] Its location has been variously attributed to (a) simultaneous metal and oxygen deficiency in $Li_{1+x}CoO_2$;[36] (b) tetrahedral site occupation in $Li[Li_{(1-2x)/3}Mn_{(2-x)/3}Ni_x]O_2$;[37] (c) *assumed* location in the metal octahedral layers of $Li[Li_x(Co_{1/3}Ni_{1/3}Mn_{1/3})_{1-x}]O_2$ with charge compensation by partial oxidation of Ni^{2+} ($Ni^{2+} = Li^+ + Ni^{3+}$);[35] and (d) excess Li salts on the oxide surface.[38]

Our XPS studies of the three compositions suggest that a small degree of lithium "overstoichiometry" in our materials is primarily the result of excess Li carbonate and hydroxide on the oxide surface, although high degrees of overstoichiometry probably result in some $Ni^{2+} \rightarrow Ni^{3+}$ oxidation. Figure 1 shows the spectra obtained for the O 1s and C 1s core peaks of compositions determined to be $Li_{1.05}Co_{1/3}Ni_{1/3}Mn_{1/3}O_2$, $Li_{1.16}Co_{1/3}N_{1/3}Mn_{1/3}O_2$, and $Li_{1.27}Co_{1/3}Ni_{1/3}Mn_{1/3}O_2$. The Ni^{3+} content as determined by oxidation state analysis of $Li_{1.05}Co_{1/3}Ni_{1/3}Mn_{1/3}O_2$ was low or negligible, whereas the other two materials exhibited 10−20% Ni^{3+} content. The

(35) Todorov, Y. M.; Numata, K. *Electrochim. Acta* **2004**, *50*, 495.
(36) Carewska, M.; Scaccia, S.; Croce, F.; Arumugam, S.; Wang, Y.; Greenbaum, S. *Solid State Ionics* **199**7, *93*, 227.
(37) Grey, C. P.; Yoon, W.-S.; Reed, J.; Ceder, G. *Electrochem. Solid-State Lett.* **2004**, *7*, A290.
(38) Pereira, N.; Matthias, C.; Bell, K.; Badway, F.; Plitz, I.; Al-Sharab, J.; Cosandey, F.; Shah, P.; Isaacs, N.; Amatuccia, G. G. *J. Electrochem. Soc.* **2005**, *152*, A114−A125.

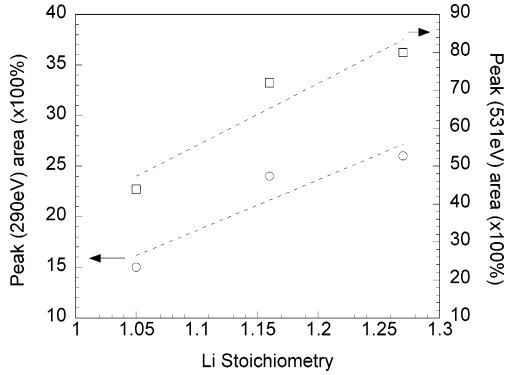

Figure 2. Relationship between Li overstoichiometry of the three compositions in Figure 1 and the areas of the C 1s peak at 290 eV and the O 1s peak at 531 eV.

main carbon C 1s peak at 285 eV (Figure 1, left) arises from "adventitious carbon". The small peak at 290 eV is associated with carbonate species on the surface of the oxides, whereas the shoulder of the main peak at 286.5 eV is assigned to hydroxyl (COH) containing species.[39] We presume that Li_2O formed as a second phase slowly converts to amorphous Li_2CO_3 after reaction with air, LiOH being an intermediate. These species are also clearly visible in the O 1s spectra (Figure 1, right), where deconvolution reveals two oxygen environments. The peak on the right recorded at 529.5 eV is assigned to the O^{2-} ions in the metal oxide framework. The peak at 531.5 eV is assigned to Li_2CO_3 or LiOH on the surface, characteristic of contaminants in metal oxides.[40] Furthermore, the ratio of the surface carbonate (as determined from the C 1s 290 eV peak or O 1s 531.5 eV peak) scales directly with respect to lithium overstoichiometry (Figure 2).

The metal 2p regions were also examined (not shown). In all cases, the Mn and Co spectra exhibited $2p_{3/2}$ peaks at 642 eV and 780 eV, respectively, which are characteristic of the 4+ and 3+ oxidation states of these metals in oxides, as expected.[39] The close similarity in binding energy between the $2p_{3/2}$ Ni^{2+} (854.8 eV) and Ni^{3+} (855.8 eV) contributions means that distinguishing between them is nontrivial; however, the most "stoichiometric" of the compositions, $Li_{1.05}Co_{0.33}Ni_{0.33}Mn_{0.34}O_2$, revealed a single peak at 854.9 eV that was fitted with a pure Gaussian line shape. Although this does not allow us to determine whether all of the excess lithium is on the surface, because there is no evidence of excess lithium occupation within the M−O layers or a second phase in the neutron diffraction data (see below) it strongly suggests that excess lithium is present as a surface contaminant for this most stoichiometric composition. The more overstoichiometric compositions displayed a Ni $2p_{3/2}$ feature that could be deconvoluted into two contributions arising from Ni^{2+} and Ni^{3+}, although accurate quantification was not possible because of the overlapped bands.

The composition $Li_{1.06}Co_{0.33}Ni_{0.33}Mn_{0.34}O_2$ (henceforth referred to as $LiCo_{1/3}Ni_{1/3}Mn_{1/3}O_2$) exhibited a homogeneous

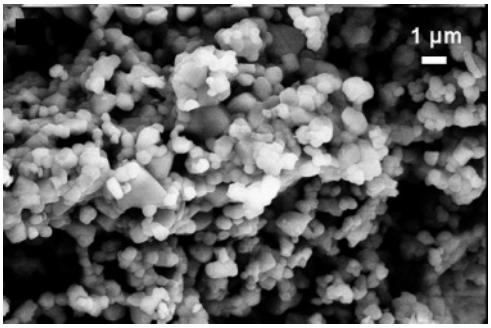

Figure 3. FESEM micrograph of $LiCo_{1/3}Ni_{1/3}Mn_{1/3}O_2$ used in the neutron diffraction studies.

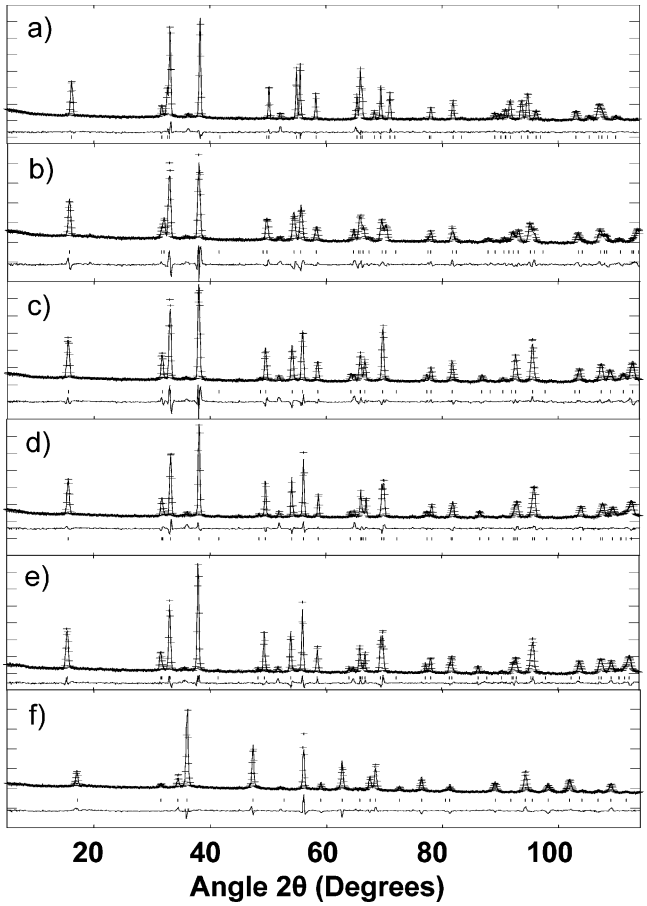

Figure 4. Rietveld refinements of powder neutron patterns of $Li_xCo_{1/3}Ni_{1/3}Mn_{1/3}O_2$ with (a) $x = 1.0$, (b) $x = 0.84$, (c) $x = 0.60$, (d) $x = 0.52$, (e) $x = 0.45$, and (f) $x = 0.04$. The experimental (+) and calculated (−) data are shown, with *hkl* positions (|) labeled.

crystallite size of about 0.5 μm as determined by FESEM (Figure 3). The neutron diffraction pattern, together with the results of Rietveld refinement, is shown in Figure 4a. The structure was refined with good agreement factors in the rhombohedral $R\bar{3}m$ space group ("O3" phase) and yielded a very low degree of cation (Li^+/Ni^{2+}) disorder (2.6%; Table 1). Attempts to refine Li exchange with elements other than Ni^{2+} (i.e., Co^{3+} or Mn^{4+}) yielded higher convergence values, as did refinements with substitution of the metal octahedral sites (3b) for lithium. Refinements in lower symmetry space groups such as $P3_112$ (see below) yielded only slightly better agreement factors. The lattice parameters $a = 2.85968(3)$ Å, $c = 14.2274(2)$ Å, and $V = 100.761(3)$ Å^3 (Table 1), from the combined neutron and X-ray refinement, are in

(39) Moulder, J. F.; Stickle, W. F.; Sobol, P. E.; Bomben, K. D.; Chastain, J. *Handbook of X-ray Photoelectron Spectroscopy*, Perkin-Elmer Corp.: Eden Prairie, MN, 1992.
(40) Shaju, K. M.; Ramanujachary, K. V.; Lofland, S. E.; Subba Rao, G. V.; Chowdari, B. V. R. *J. Mater. Chem.* **2003**, *13*, 2633.

Table 1. Summary of $LiCo_{1/3}Ni_{1/3}Mn_{1/3}O_2$ Refinement (Neutron Data)

Cell Parameters

space group $R\bar{3}m$
$a = 2.860(2)$ Å; $c = 14.227(8)$ Å; $V = 100.76(9)$ Å^3; $Z = 3$

Atomic Positions

name	*x*	*y*	*z*	$U \times 100$	fract	site
Li	0.00000	0.00000	0.00000	0.012(3)	0.975(1)	3a
Co	0.00000	0.00000	0.50000	0.007(1)	0.3333	3b
Ni	0.00000	0.00000	0.50000	0.007(1)	0.309(1)	3b
Mn	0.00000	0.00000	0.50000	0.007(1)	0.3333	3b
O	0.00000	0.00000	0.2411(1)	0.008(1)	1.0000	6c
Li-d	0.00000	0.00000	0.50000	0.012(1)	0.025(1)	3b
Ni-d	0.00000	0.00000	0.00000	0.007(1)	0.025(1)	3a

Refinement Parameters

angular range = 5−114°; number of variables = 22
constraints: $u_{iso}(Co) = U_{iso}(Ni) = U_{iso}(Mn) = U_{iso}(Ni\text{-}d)$
$U_{iso}(Li) = U_{iso}(Li\text{-}d)$
frac(Li) + frac(Li-d) = 1.0; frac(Ni) + frac(Ni-d) = 0.3333
$R_{wp} = 2.95\%$; $\chi^2 = 5.868$; $R_{F2} = 15.43\%$

Selected Interatomic Distances (Å)

Li−O	2.1048(9)
M−O	1.9615(7)

Table 2. Summary of $Li_{0.84}Co_{1/3}Ni_{1/3}Mn_{1/3}O_2$ Refinement (Neutron Data)

Cell Parameters

space group $R\bar{3}m$
$a = 2.8313(2)$ Å; $c = 14.310(2)$ Å; $V = 99.34(2)$ Å^3; $Z = 3$

Atomic Positions

name	*x*	*y*	*z*	$U \times 100$	fract	site
Li	0.00000	0.00000	0.00000	0.013(4)	0.83(4)	3a
Co	0.00000	0.00000	0.50000	0.008(2)	0.3333	3b
Ni	0.00000	0.00000	0.50000	0.008(2)	0.298(7)	3b
Mn	0.00000	0.00000	0.50000	0.008(2)	0.3333	3b
O	0.00000	0.00000	0.2392(2)	0.012(1)	1.0000	6c
Li-d	0.00000	0.00000	0.50000	0.013(4)	0.0000	3b
Ni-d	0.00000	0.00000	0.00000	0.008(2)	0.036(7)	3a

Refinement Parameters

angular range = 5−116°; number of variables = 23
constraints: $u_{iso}(Co) = U_{iso}(Ni) = U_{iso}(Mn) = U_{iso}(Ni\text{-}d)$
$U_{iso}(Li) = U_{iso}(Li\text{-}d)$
frac(Ni) + frac(Ni-d) = 0.3333
$R_{wp} = 5.14\%$; $\chi^2 = 6.858$; $R_{F2} = 8.42\%$

Selected Interatomic Distances (Å)

Li−O	2.1182(18)
M−O	1.9363(15)

excellent accord with those reported by Ohzuku and Yabuuchi from XRD lattice refinements ($a = 2.862(2)$, $c = 14.227(8)$, and $V = 100.6$ Å^3).[13] This confirms the composition of the pristine material. The Li−O bond distance (2.11 Å) is identical to that of $LiNiO_2$, and the metal−oxygen bond distance (average of 1.96 Å) lies between $LiCoO_2$ (1.92 Å)[41] and $LiNiO_2$ (1.97 Å).[42] Structurally, $LiCo_{1/3}Ni_{1/3}Mn_{1/3}O_2$ resembles $LiNiO_2$ more closely because both materials have cation disorder.

The presence of three metal cations of different valency within a trigonal lattice suggests they may adopt a special arrangement. A superlattice of $LiCo_{1/3}Ni_{1/3}Mn_{1/3}O_2$ has been predicted by Koyama et al., consisting of the Ni, Mn, and Co ions ordered to form a supercell of symmetry $P3_112$.[43] Recent calculations indicate that its total stabilization energy relative to the sum of the three component layered oxides is between −0.129 and −0.168 eV per formula unit, and its formation would be weakly thermodynamically favorable.[44] If such ordering were long-range and persists along the *c* axis, it would be visible by PND as a result of the high contrast of scattering lengths of these transition metals (Ni, 14.4 fm; Mn, −3.73 fm; Co, 2.49 fm; Li, −1.90 fm). Very recent reports by others do not detail its existence, however,[45,46] and we also failed to uncover additional superlattice reflections either in this composition or in the others that we examined. This may be a consequence of the Li/Ni exchange, which could disrupt long-range metal cation ordering even at the very low levels of exchange that we observed for our materials, of 2−3%. The superstructure reflections in hypothetical ordered $LiNi_{1/2}Mn_{1/2}O_2$ disappear when the Li/Ni exchange reaches the experimentally observed level of ∼10%.[47] Short-range superlattice order probably still exists, however, and evidence for this has been recently demonstrated by local probe (short-range) techniques such as ^{7}Li magic-angle spinning (MAS) NMR.[48] Recently, it was also reported that compositions $LiCo_{1/3}Ni_{1/3}Mn_{1/3}O_2$ give better refinements in the $P3_112$ space group and that this may be indicative of in-plane superlattice order although long-range order cannot be seen by diffraction.[49] Nonetheless, refinements in a lower symmetry usually provide slightly better statistics. Resolution of this issue may be ultimately attained using techniques such as selected area diffraction.

II. Neutron Diffraction Studies of the Delithiated Phases, $Li_{1-x}Co_{1/3}Ni_{1/3}Mn_{1/3}O_2$. Delithiated samples were prepared by chemical oxidation, allowing the preparation of bulk quantities of delithiated samples that are free of electrolyte.[50] An excess of NO_2BF_4 oxidant was needed to obtain the desired level of lithium extraction, as shown in Figure 5. The neutron refinements of the delithiated phases corresponding to the $Li_{1-x}Co_{1/3}Ni_{1/3}Mn_{1/3}O_2$ ($1 - x = 0.84$, 0.60, 0.54, and 0.45) compositions are presented in Figure 4b−e and summarized in Tables 2−5. The $R\bar{3}m$ symmetry is maintained throughout. We observed a slight decrease in the *a* axis from 2.8562 to 2.8173 Å and an increase in the *c* axis from 14.2214 to 14.534 Å compared to the starting compound (Figure 6). This gives rise to an overall decrease in cell volume, of only 1% at $x = 0.45$. The *unconstrained* refined lithium occupancies in the lithium layer (3a site) are in excellent agreement with the ICP results for all values of $1 - x$ (Tables 2−5: $1 - x = 0.84$ for ICP and 0.83 refined; $1 - x = 0.60$ from ICP and 0.63 refined; $1 - x = 0.52$ from ICP and 0.58 refined; and $1 - x = 0.45$ from ICP and 0.48

(41) Akimoto, J.; Gotoh, Y.; Oosawa, Y. *J. Solid State Chem.* **1998**, *141*, 298.
(42) Croguennec, L.; Pouillerie, C.; Delmas, C. *J. Electrochem. Soc.* **2000**, *147*, 1314.
(43) Koyama, Y.; Tanaka, I.; Adachi, H.; Makimura, Y.; Ohzuku, T. *J. Power Sources* **2003**, *119*−*121*, 644.
(44) Koyama, Y.; Yabuuchi, N.; Tanaka, I.; Adachi, H.; Ohzuku, T. *J. Electrochem. Soc.* **2004**, *151*, A1545.
(45) Kim, J.-M.; Chung, H.-T. *Electrochim. Acta* **2004**, *49*, 937.
(46) Whitfield, P. S.; Davidson, I. J.; Cranswick, L. M. D.; Swainson, I. P.; Stephens, P. W. *Solid State Ionics* **2005**, *176*, 463.
(47) Meng, Y. S.; Ceder, G.; Grey, C. P.; Yoon, W.-S.; Shao-Horn, Y. *Electrochem. Solid-State Lett.* **2004**, *7*, A155.
(48) Cahill, L. S.; Samoson, A.; Yin, S.-C.; Nazar, L. F.; Goward, G. R. *Chem. Mater.* **2005**, *17*, 6560.
(49) Yabuuchi, N.; Koyama, Y.; Nakayama, N.; Ohzuku, T. *J. Electrochem. Soc.* **2005**, *152*, A1434.
(50) Yin, S.-C.; Grondey, H.; Strobel, P.; Anne, M.; Nazar, L. F. *J. Am. Chem. Soc.* **2003**, *125*, 10402.

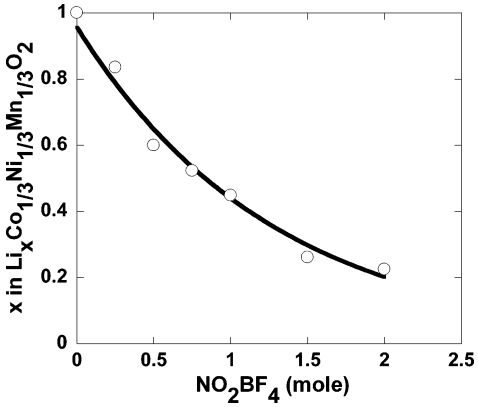

Figure 5. Relationship between the concentration of oxidant NO_2BF_4 used for delithiation of $LiCo_{1/3}Ni_{1/3}Mn_{1/3}O_2$ and the resultant lithium stoichiometry, as determined by ICP.

Table 3. Summary of $Li_{0.60}Co_{1/3}Ni_{1/3}Mn_{1/3}O_2$ Refinement (Neutron Data)

Cell Parameters

space group $R\bar{3}m$
$a = 2.8220(2)$ Å; $c = 14.463(1)$ Å; $V = 99.74(1)$ Å^3; $Z = 3$

Atomic Positions

name	*x*	*y*	*z*	$U \times 100$	fract	site
Li	0.00000	0.00000	0.00000	0.022(4)	0.63(4)	3a
Co	0.00000	0.00000	0.50000	0.011(2)	0.3333	3b
Ni	0.00000	0.00000	0.50000	0.011(2)	0.296(6)	3b
Mn	0.00000	0.00000	0.50000	0.011(2)	0.3333	3b
O	0.00000	0.00000	0.2367(2)	0.0121(5)	1.0000	6c
Li-d	0.00000	0.00000	0.50000	0.022(4)	0.0000	3b
Ni-d	0.00000	0.00000	0.00000	0.011(2)	0.037(6)	3a

Refinement Parameters

angular range = 5−116°; number of variables = 23
constraints: $u_{iso}(Co) = U_{iso}(Ni) = U_{iso}(Mn) = U_{iso}(Ni\text{-}d)$
$U_{iso}(Li) = U_{iso}(Li\text{-}d)$
frac(Ni) + frac(Ni-d) = 0.3333
$R_{wp} = 4.57\%$; $\chi^2 = 15.47$; $R_{F2} = 7.37\%$

Selected Interatomic Distances (Å)

Li−O	2.1463(15)
M−O	1.9187(12)

refined). Thus, we are confident of the precision of the chemical delithiation method to target specific lithium compositions, once the relationship between the desired ratio of oxidant/oxide is established.

Attempts to refine occupancy on the disordered lithium (3b site, in the transition metal layers) led to unstable refinements, possibly due to the small amount of lithium present and its small scattering length (−2.2 fm). We presume that lithium in this site may be extracted on delithiation, based on MAS NMR studies that show lithium ions are gradually removed from *both* sites (in the Li and in the metal layer): complete removal of lithium residing in the metal layers occurs between $x = 0.4-0.6$ in $Li_{1-x}Co_{1/3}Ni_{1/3}Mn_{1/3}O_2$.[51] In contrast, the occupancy refinement on the Ni disorder site (3a) is relatively stable due to its high scattering length (14.4 fm). The degree of Ni occupancy in these sites remained essentially constant (∼3.0−3.6%) upon delithiation. As in the starting compound, occupancy of this site with Co^{3+} or Mn^{4+} led to unreasonable thermal factors.

(51) Yoon, W.-S.; Grey, C. P.; Balasubramanian, M.; Yang, X.-Q.; Fischer, McBreen, D. A. J. *Electrochem. Solid-State Lett.* **2004**, *7*, A53.

Table 4. Summary of $Li_{0.52}Co_{1/3}Ni_{1/3}Mn_{1/3}O_2$ Refinement (Neutron Data)

Cell Parameters

space group $R\bar{3}m$
$a = 2.8187(1)$ Å; $c = 14.5305(8)$ Å; $V = 99.98(1)$ Å^3; $Z = 3$

Atomic Positions

name	*x*	*y*	*z*	$U \times 100$	fract	site
Li	0.00000	0.00000	0.00000	0.024(4)	0.58(3)	3a
Co	0.00000	0.00000	0.50000	0.003(1)	0.3333	3b
Ni	0.00000	0.00000	0.50000	0.003(1)	0.300(4)	3b
Mn	0.00000	0.00000	0.50000	0.003(1)	0.3333	3b
O	0.00000	0.00000	0.2361(1)	0.0083(6)	1.0000	6c
Li-d	0.00000	0.00000	0.50000	0.022(4)	0.0000	3b
Ni-d	0.00000	0.00000	0.00000	0.003(1)	0.033(4)	3a

Refinement Parameters

angular range = 5−114°; number of variables = 23
constraints: $u_{iso}(Co) = U_{iso}(Ni) = U_{iso}(Mn) = U_{iso}(Ni\text{-}d)$
$U_{iso}(Li) = U_{iso}(Li\text{-}d)$
frac(Ni) + frac(Ni-d) = 0.3333
$R_{wp} = 3.23\%$; $\chi^2 = 7.846$; $R_{F2} = 5.72\%$

Selected Interatomic Distances (Å)

Li−O	2.1554(10)
M−O	1.9145(8)

Table 5. Summary of $Li_{0.45}Co_{1/3}Ni_{1/3}Mn_{1/3}O_2$ Refinement (Neutron Data)

Cell Parameters

space group $R\bar{3}m$
$a = 2.8173(2)$ Å; $c = 14.534(1)$ Å; $V = 99.90(1)$ Å^3; $Z = 3$

Atomic Positions

name	*x*	*y*	*z*	$U \times 100$	fract	site
Li	0.00000	0.00000	0.00000	0.028(5)	0.48(3)	3a
Co	0.00000	0.00000	0.50000	0.005(1)	0.3333	3b
Ni	0.00000	0.00000	0.50000	0.005(1)	0.298(4)	3b
Mn	0.00000	0.00000	0.50000	0.005(1)	0.3333	3b
O	0.00000	0.00000	0.2354(1)	0.0094(5)	1.0000	6c
Li-d	0.00000	0.00000	0.50000	0.028(5)	0.0000	3b
Ni-d	0.00000	0.00000	0.00000	0.005(1)	0.035(4)	3a

Refinement Parameters

angular range = 5−116°; number of variables = 23
constraints: $u_{iso}(Co) = U_{iso}(Ni) = U_{iso}(Mn) = U_{iso}(Ni\text{-}d)$
$U_{iso}(Li) = U_{iso}(Li\text{-}d)$
frac(Ni) + frac(Ni-d) = 0.3333
$R_{wp} = 3.81\%$; $\chi^2 = 3.874$; $R_{F2} = 6.50\%$

Selected Interatomic Distances (Å)

Li−O	2.1611(10)
M−O	1.9091(8)

Over the range of $1 - x = 0.84-0.45$, the Li−O bond distance gradually increases by comparison to the starting material (to 2.16 Å from 2.11 Å), and the *average* metal−oxygen bond gradually decreases to 1.91 Å (Tables 1 and 2−5). For $1 - x = 0.60$, the lithium−oxygen and metal−oxygen bond distances are very comparable to the distances in $LiCoO_2$. This is mainly due to oxidation of Ni^{2+} (0.69 Å) to Ni^{3+} (0.60 Å). The interlayer distance between the metal oxide slabs increases slightly as a consequence of decreasing the electrostatic attraction between lithium and oxygen upon lithium removal.

III. Formation of the O1 Phase: $Li_xCo_{1/3}Ni_{1/3}Mn_{1/3}O_2$, $x = 0.30-0$. Formation of an O1 phase upon deep extraction of lithium from layered O3 lithium metal oxides has been reported for a few materials, including $LiCoO_2$ where it was first observed.[52,53] The O1 phase encompasses only one MO_2 unit along the *c* axis and, clearly, vacancies in the Li−O layer. The unit cell contains metal cations and oxygen located

Table 6. Summary of $Li_{0.04}Co_{1/3}Ni_{1/3}Mn_{1/3}O_2$ Refinement (Neutron Data)

Cell Parameters

space group $P\bar{3}m1$
$a = 2.8269(4)$ Å; $c = 4.4894(6)$ Å; $V = 31.070(7)$ Å^3; $Z = 1$

Atomic Positions

name	*x*	*y*	*z*	$U \times 100$	fract	site
Co	0.00000	0.00000	0.00000	0.007(1)	0.3333	1a
Ni	0.00000	0.00000	0.00000	0.007(1)	0.307(4)	1a
Mn	0.00000	0.00000	0.00000	0.007(1)	0.3333	1a
O	0.33333	0.66666	0.2186(5)	0.008(1)	1.0000	2d
Ni-d	0.00000	0.00000	0.50000	0.007(1)	0.026(4)	1b

Refinement Parameters

angular range = 5−114°; number of variables = 22
constraints: $u_{iso}(Co) = U_{iso}(Ni) = U_{iso}(Mn) = U_{iso}(Ni\text{-}d)$
frac(Ni) + frac(Ni-d) = 0.3333
$R_{wp} = 3.65\%$; χ^2=28.18; $R_{F2} = 8.93\%$

Selected Interatomic Distances (Å)

M−O	1.9044(12)
Ni-d−O	2.0640(14)

at the 1a and 2d sites, respectively, with symmetry reduced from rhombohedral to trigonal ($P\bar{3}m1$; space group 164).[20,54] For $LiNiO_2$, the end product O1 phase symmetry was reported to be either monoclinic[55] or trigonal $P\bar{3}m1$.[42] In $Li_{1-x}Co_{1/3}Ni_{1/3}Mn_{1/3}O_2$, the O1 phase first appears at oxidation levels beyond $1 - x = 0.45$, becoming evident at about $1 - x = 0.30$. Complete delithiation of $LiCo_{1/3}Mn_{1/3}Ni_{1/3}O_2$ (Figure 7a) results in formation of a pure O1 phase (Figure 7b). If de-intercalation is limited to the stoichiometry $Li_{0.26}Co_{1/3}Ni_{1/3}Mn_{1/3}O_2$, the O1 phase is clearly visible as a minor component as shown in the XRD pattern in Figure 7d. The pattern was refined with two phases, with an O3/O1 phase fraction of 0.8:0.2. The majority O3 phase displayed lattice constants close to $Li_{0.45}Co_{1/3}Ni_{1/3}Mn_{1/3}O_2$ ($a = 2.8210(1)$, $c = 14.406(1)$), and the O1 phase exhibited lattice constants of $a = 2.8261(5)$ Å, $c = 4.544(1)$ Å, and oxygen at (1/3, 2/3, 0.3132). This indicates that the Li stoichiometry of the O1 phase is very low or close to zero. We note that at this level of lithium extraction (∼75%), the two-phase transformation is just underway. Undoubtedly some regions of the crystallite convert to the O1 phase, whereas others may be inhibited from doing so by defects within the structure that impede the "slippage" necessary to accommodate the reaction. However, we cannot rule out the possibility that the transformation is a function of particle size. Therefore, some small fraction of crystallites undergoes conversion more completely at intermediate degrees of lithium extraction. We did not see evidence of an additional or intermediate low-lithium phase in either XRD or PND patterns of our low-lithium materials, such as observed in early reports of delithiation of Li_xCoO_2 at $x \approx 0.18-0.21$.[52] The chemical delithiation method makes it difficult to precisely control the stoichiometry to target the formation of this phase (see below for further discussion).

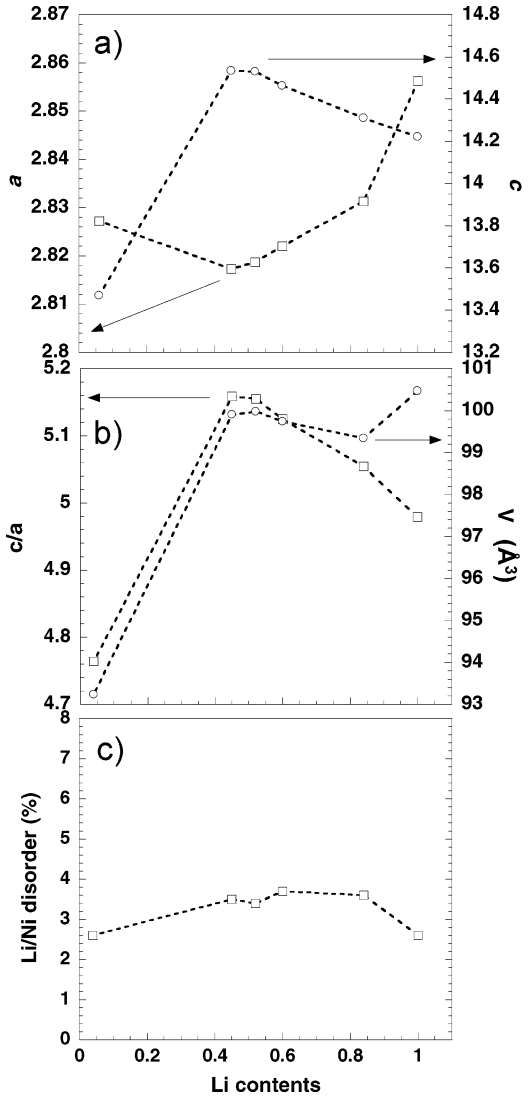

Figure 6. Lattice constants *a* and *c* (a), the *c*/*a* ratio, *V* (b), and the degree of disorder (c) of $Li_xCo_{1/3}Ni_{1/3}Mn_{1/3}O_2$ samples prepared by chemical delithiation.

Figure 4f displays the PND pattern of an essentially fully delithiated composition ($Li_{0.04}Co_{1/3}Ni_{1/3}Mn_{1/3}O_2$, by ICP). The results of the Rietveld refinement (Table 6) show that $Li_{0.04}Co_{1/3}Ni_{1/3}Mn_{1/3}O_2$ is a single phase that exhibits the same trigonal O1 structure as found for CoO_2 and NiO_2.[42] Its lattice parameters ($a = 2.827$ Å, $c = 4.489$ Å) and fractional coordinates for oxygen (1/3, 2/3, 0.219) are very similar to the minor O1 phase observed in the $Li_{0.26}Co_{1/3}Ni_{1/3}Mn_{1/3}O_2$ composition in Figure 7d. Refinement of the oxygen fractional occupancy did not lead to values significantly different than one, suggesting that oxygen is not removed from the lattice under deep oxidation to an appreciable degree under these conditions. This has important ramifications for the safety of the material, vis a vis $Li_{1-x}CoO_2$, which is

Table 7. Structure Summary of Delithiated $Li_{1-x}Co_{1/3}Ni_{1/3}Mn_{1/3}O_2$ Samples by Chemical Oxidation

Li: [1 − *x*]	*a* (Å)	c (Å)	*V* (Å^3)	diso. (%)	Li occu.	$O_{(z)}$	R_{wp} (%)	X^2	R_b (%)
1	2.8562(2)	14.2214(8)	100.473(9)	2.6(2)	1	0.2414(1)	2.95	5.868	15.43
0.84	2.8313(2)	14.310(2)	99.342(2)	3.6(7)	0.83	0.2392(2)	5.14	6.858	8.42
0.6	2.8220(2)	14.463(1)	99.74(1)	3.7(6)	0.63	0.2367(2)	4.57	15.47	7.37
0.52	2.8187(1)	14.5305(8)	99.98(1)	3.4(4)	0.58	0.2361(1)	3.23	7.846	5.72
0.45	2.8173(2)	14.534(1)	99.90(1)	3.5(4)	0.48	0.2354(1)	3.81	3.874	6.5
0.04	2.8269(4)	4.4894(6)	31.070(7)	2.6(4)		0.2168(5)	3.65	28.18	8.93

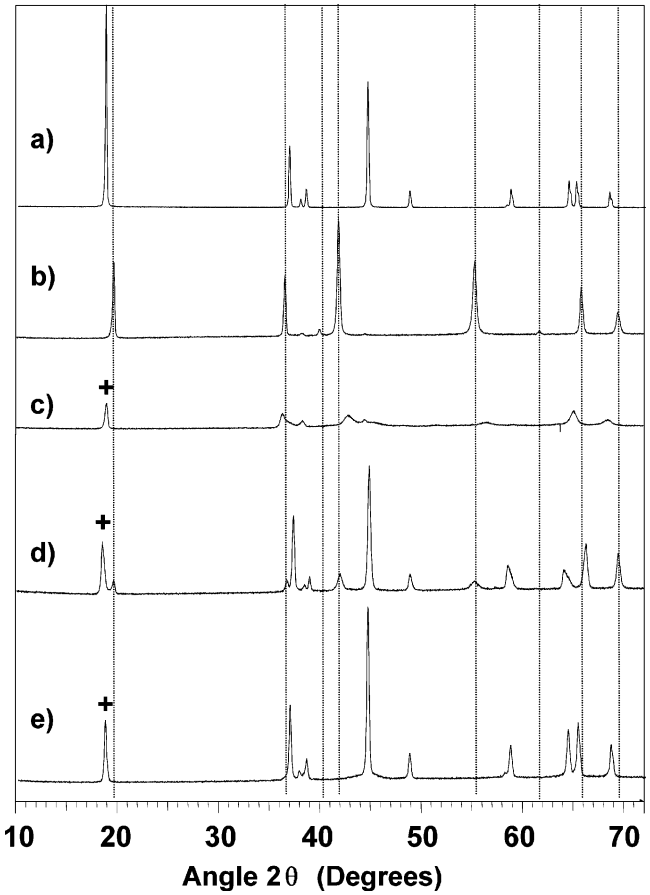

Figure 7. XRD patterns of $LiCo_{1/3}Ni_{1/3}Mn_{1/3}O_2$: (a) starting phase, (b) delithiated by 150% excess NO_2BF_4 to give $Li_{0.04}Co_{1/3}Ni_{1/3}Mn_{1/3}O_2$, (c) relithiated by 300% excess LiI, (d) delithiated to give $Li_{0.26}Co_{1/3}Ni_{1/3}Mn_{1/3}O_2$, and (e) composition in part d relithiated by 300% excess LiI to give $Li_{1.02}Co_{1/3}Ni_{1/3}Mn_{1/3}O_2$. The dotted line indicates reflections of the O1 phase, and decreased intensities (+) at low angle (~20° 2θ) for delithited and relithiated materials are due to the air sensitive holder geometry.

reported to lose oxygen at electrochemical extraction limits as low as 0.5.[56]

Although the changes in lattice parameter and cell volume are very small within the O3 phase range, upon full extraction, the *c* axis of the cell contracts as much as 5.3% compared to the starting material (this value is multiplied by three to account for the difference in the stacking order), and cell volume is decreased by 7.2%. It leads to irreversibility on subsequent reduction: namely, difficulty in transforming the O1 structure back to the O3 phase, as described in the next section. This factor could be responsible for the cracking of the electrode composite at high cutoff voltages. Lattice parameters for the delithiated phases are summarized in Figure 6 and Table 7.

The formation of the O1 phase originates from the gliding of metal oxide layer slabs in the O3 phase after Li removal, as first described for Li_xNiO_2,[57] and is driven by minimization

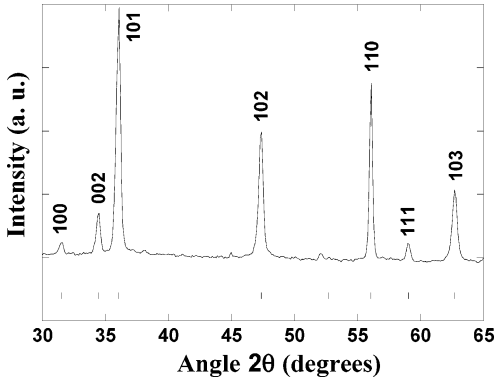

Figure 8. Magnification of Figure 4f which shows the broadening of 10*l* reflections in $Li_{0.04}Co_{1/3}Ni_{1/3}Mn_{1/3}O_2$.

of oxygen p orbital interactions adjacent to the van der Waals gap. As a result of a small fraction of disordered nickel cations in the interslab space of Li_xNiO_2, the ideal O1 phase packing (AB) is not attainable, resulting in a small amount of O3 stacking faults (ABC).[57] Simulations of Li_xNiO_2 diffraction patterns showed that the broadening of the (10*l*) reflections depend on the relative fraction of the stacking faults and, hence, the degree of disorder.[57] The (101), (102), and (103) lines in $Li_{0.04}Co_{1/3}Ni_{1/3}Mn_{1/3}O_2$ are also slightly broadened compared to other reflections (Figure 8), consistent with the small degree of Ni site occupation on the 3a sites (see above). The difference Fourier map revealed that residual electron density was located at (0, 0, 1/2), which corresponds to the 3% Ni disorder located in the refinement.

IV. Reversibility of Lithium Re-Intercalation To Form $LiCo_{1/3}Ni_{1/3}Mn_{1/3}O_2$. The $Li_{0.04}Co_{1/3}Ni_{1/3}Mn_{1/3}O_2$ shown above in Figure 7b was chemically relithiated using a 300% excess of LiI, to explore the reversibility of transformation back to the O3 phase. The XRD pattern (Figure 7c) reveals that the crystalline O3 structure is not formed on re-intercalation of lithium. A satisfactory refinement of the pattern could not be obtained based on the O3 structure, a mixture of the O1 and O3 phase, nor the related P3 structure. In contrast, $LiCo_{1/3}Ni_{1/3}Mn_{1/3}O_2$ that was only delithiated to a composition of $Li_{0.26}Co_{1/3}Ni_{1/3}Mn_{1/3}O_2$ as described in the previous section (giving rise to about 19% of the O1 phase) could be readily re-intercalated to form a single crystalline O3 phase with $R\bar{3}m$ symmetry and composition as determined from ICP of $Li_{1.02}Co_{1/3}Ni_{1/3}Mn_{1/3}O_2$ (Figure 7e). The lattice constants ($a = 2.852$ Å and $c = 14.262$ Å) are very close to the starting material. Consistent with these observations, samples that were subjected to an intermediate degree of delithiation to form a majority O1 phase (although not as a pure single phase) exhibited partial conversion to the O3 phase as shown in Figure 9. The XRD patterns of the (a) starting phase, (b) partially delithiated material, and relithiated materials using LiI in molar ratios of 35% (c), 65% (d), and 100% (e) are depicted. The lattice parameters of the O1 phase ($a = 2.828$, $c = 4.516$) in Figure 9 are very close to those of the pure O1 phase described above. The breadth and shape of the reflections in Figures 7c and 9e also indicate the presence of a very high degree of stacking

(52) Amatucci, G. G.; Tarascon, J. M.; Klein, L. C. *J. Electrochem. Soc.* **1996**, *143*, 1114.
(53) Venkatraman, S.; Choi, J.; Manthiram, A. *Electrochem. Comm.* **2004**, *6*, 832.
(54) Manthiram, A.; Venkatraman, S. *Chem. Mater.* **2002**, *14*, 3907.
(55) Tarascon, J. M.; Vaughan, G.; Chabre, Y.; Seguin, L.; Anne, M.; Strobel, P.; Amatucci, G. *J. Solid State Chem.* **1999**, *147*, 410.
(56) Venkatraman, S.; Shin, Y.; Manthiram, A. *Electrochem. Solid-State Lett.* **2003**, *6*, A9.
(57) Croguennec, L.; Pouillerie, C.; Mansour, A. N.; Delmas, C. *J. Mater. Chem.* **2001**, *11*, 131.

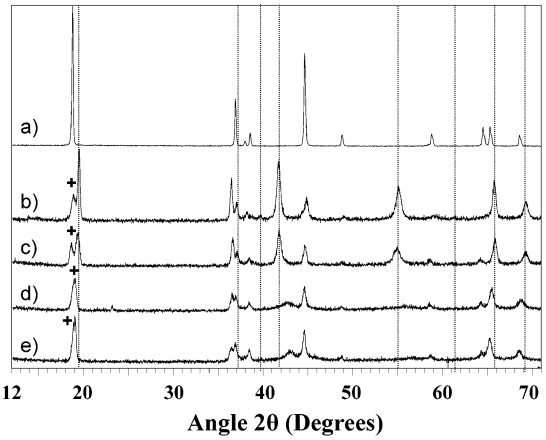

Figure 9. Study of the effect of the extent of delithiation−relithiation: XRD patterns of (a) the starting phase, $LiCo_{1/3}Ni_{1/3}Mn_{1/3}O_2$, (b) delithiated to give $\sim Li_{0.15}Co_{1/3}Ni_{1/3}Mn_{1/3}O_2$, and relithiated by (c) 35% LiI, (d) 65% LiI, and (e) 100% LiI. The dotted line denotes the fully delithiated O1 phase, and decreased intensities (+) at low angle due to the air sensitive holder geometry are labeled.

faults, which are particularly severe in Figure 9e and most prominent in Figure 7c. These are generated by inhibited nucleation of local domains of the O3 phase within the O1 phase on re-intercalation as a result of irreversible O1 to O3 transformation.

The electrochemical behavior of $LiCo_{1/3}Ni_{1/3}Mn_{1/3}O_2$ is in complete accord with chemical delithiation−relithiation. The voltage−capacity curves in different voltage windows that vary according to cutoff potential (4.4−4.8 V) are shown in Figure 10a), and the data are summarized in Table 8. The cell cycled to 4.4 V exhibits moderate extraction of 0.64 Li (180 mA h g^{-1}) on first charge, with 13.8% irreversible capacity loss on the first cycle. Capacity retention is relatively good in this window. As the upper cutoff voltage is increased, the irreversible capacity loss increases and the capacity retention sharply decreases. An upper cutoff voltage of 4.8 V results in almost complete extraction of the material (0.91 Li, 252.1 mA h g^{-1}) but also leads to very rapid capacity fading as illustrated in Figure 10b). This fading is not due to electrolyte oxidation, as $LiPF_6$ in EC/DMC is quasi-stable up to 4.8 V. The optimum upper cutoff voltage of ≤4.6 V corresponds to the stoichiometry $Li_{1-x}Co_{1/3}Ni_{1/3}Mn_{1/3}O_2$, where transformation to the O1 phase starts to become significant, namely, at $1 - x \leq 0.25$. The latter region above 4.6 V is characterized by a gentle change in slope (evident as a broad, slightly split feature in the differential capacity dx/dV plots centered at 4.65 V), that signals the phase transition. Our C/10 rate may be sufficiently high that the transition is "smeared out" over a range of compositions, and/or it occurs at slightly different compositions within different regions in the crystallites due to local cation disorder effects.

The large fraction of stacking faults evident on complete chemical delithiation−relithiation (Figures 7c and 9e), along with the electrochemical observations described above, lead us to speculate on the nature of the transition. The O1 phase in Li_xCoO_2 is predicted to be stable only at very low lithium concentrations close to zero,[58] in accordance with our observation of its formation in $Li_{0.04}Co_{1/3}Ni_{1/3}Mn_{1/3}O_2$. This raises the question of whether the transformation of the O3

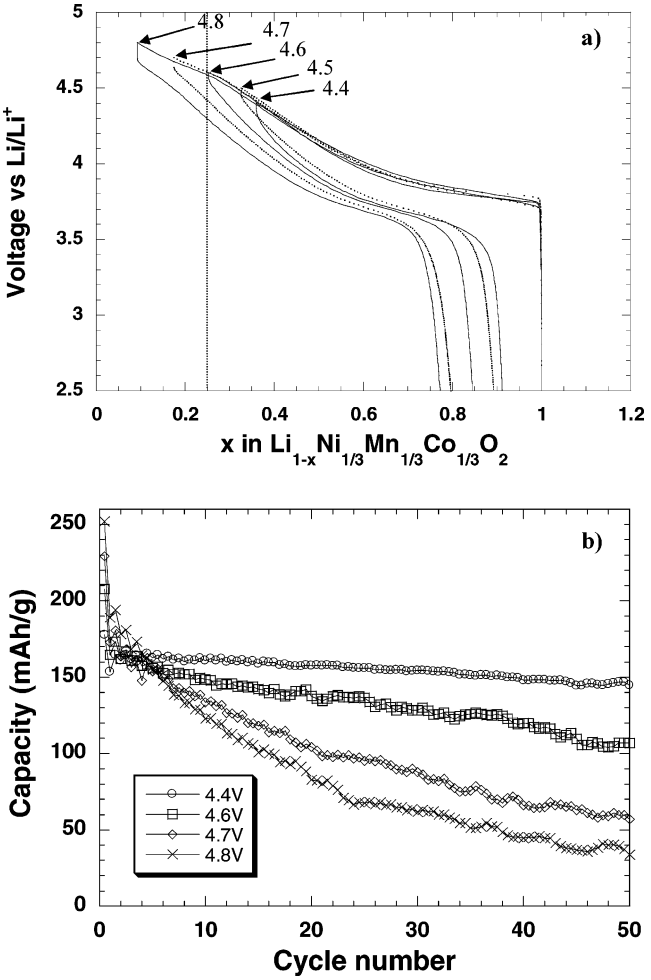

Figure 10. Electrochemical behavior of $LiCo_{1/3}Ni_{1/3}Mn_{1/3}O_2$: (a) voltage−capacity curves and (b) capacity retention on cycling to different upper cutoff voltages. The dotted line indicates the point ($x > 0.75$; a capacity of 200 mA h g^{-1}) beyond which the appearance of a second plateau becomes visible.

Table 8. Capacity as a Function of Voltage Window

cutoff voltage (V)	first charge cap. (mA h g^{-1})	irre. cap. on first cycle (mA h g^{-1})	cap. at 50 cycles
4.4	178	13.8	144.7
4.5	186	15.9	
4.6	209	20.7	106.8
4.7	231	24.7	57.0
4.8	253	25.1	33.8

to the O1 structure in the mixed metal oxide is a simple two phase reaction (which should give rise to a distinct and flat plateau in the region above 4.6 V) or whether it proceeds through an intermediate phase such as forms in Li_xCoO_2 when more than 0.75 Li are extracted from the structure.[52] This phase, designated as H1-3, was predicted and identified as a two-stage compound by first principles calculations[59] and was clearly confirmed by subsequent detailed experiments.[60] The term H1-3 refers to its hybrid nature that encompasses both the O3 and O1 stacking sequences. It was shown that de-intercalation of x (Li) < 0.25 in Li_xCoO_2 is first accompanied by an O3 → H1-3 transition, followed by

(58) Van der Ven, A.; Aydinol, M. K.; Ceder, G. *Phys. Rev. B* **1998**, *58*, 2975;
(59) Van der Ven, A.; Aydinol, M. K.; Ceder, G. *J. Electrochem. Soc.* **1996**, *145*, 2149.
(60) Chen, Z.; Lu, Z.; Dahn, J. R. *J. Electrochem. Soc.* **2002**, *149*, A1604.

an H1-3 to O1 transition, complete at $x = 0$.[60] The fact that two phase transitions are not distinctly evident in the electrochemical curve may be the result of a low level Li/Ni disorder within the $Li_{1-x}Co_{1/3}Ni_{1/3}Mn_{1/3}O_2$ compounds that either inhibits staging or precludes its ready identification. In situ XRD experiments are currently underway to investigate the low-lithium regime between $Li_{0.26}Co_{1/3}Ni_{1/3}Mn_{1/3}O_2$ and $Li_{0.04}Co_{1/3}Ni_{1/3}Mn_{1/3}O_2$ to see if such intermediate staged compounds do play a role.

Conclusions

Neutron and X-ray diffraction studies demonstrate that the extent to which $Li_{1-x}Co_{1/3}Ni_{1/3}Mn_{1/3}O_2$ is delithiated plays a role in determining the reversibility of lithium re-intercalation. A phase change from the starting O3 phase (with $R\bar{3}m$ symmetry) to the O1 phase (with $P\bar{3}m1$ symmetry) occurs at a lithium content of about $1 - x = 0.30$. For values of x lower than 0.7, lattice symmetry is preserved with a very small volume variation of only 1%, and the Ni ions within the lithium layer (3a sites) appear to remain fixed. Transformation to the O1 phase occurs beyond extraction of 0.70Li, as a result of minimizing the van der Waals gap interactions between the metal oxide slabs. The fully delithiated "$Li_{0.04}Co_{1/3}Ni_{1/3}Mn_{1/3}O_2$" O1 phase shows little evidence for substantial oxygen vacancies, but subsequent re-formation of the crystalline O3 phase is not observed on re-intercalation of lithium. In contrast, relithiation is accompanied by formation of a very large fraction of stacking faults within the layered lattice. Both partial Ni^{2+} oxidation and particle morphology/agglomeration have roles to play in the extent of the Li extraction. While Li overstoichiometric and more agglomerated materials exhibit limited O1 phase formation, re-formation of the O3 phase is readily reversible. Electrochemical studies are in accord with these observations. The cycling stability of $LiCo_{1/3}Ni_{1/3}Mn_{1/3}O_2$ up to a cutoff voltage of 4.4 V, corresponding to a phase limit of $1 - x < 0.30$, gives rise to relatively stable behavior, whereas cycling to a cutoff voltage above 4.6 V, which corresponds to $1 - x > 0.25$, leads to an increase in the irreversibility and rapid capacity fading.

Acknowledgment. L.F.N. is grateful to the NSERC for funding through their Discovery and Strategic Programs and MMO for funding through their EMK program. The authors appreciate the very helpful discussions of the research team at INCO, Inc. (Sheridan Park, Ontario), including Drs. Quan Yang, Henry Huang, Feng Zhou, and Eric Wasmund. S.-C.Y. acknowledges Dr. Lachlan M. D. Cranswick at the Chalk River Neutron Facility, Canada, for assistance with the neutron diffraction experiments.

CM0511769